PROCEEDINGS OF SCIENCE

The Large Flares of Mrk 421 in 2006: signature of electron acceleration and energetic budget of the jet

Andrea Tramacere* **ISDC, Data Centre for Astrophysics Chemin d'Ecogia 16 CH-1290 Versoix Switzerland**
E-mail: andrea.tramacere@unige.ch

We present the results of a deep spectral analysis of all Swift observations of Mrk 421 between April 2006 and July 2006, when it reached its highest X-ray flux recorded until the end of 2006. We completed this data set with other historical X-ray observations. We used the full data set to investigate the correlation between the spectral parameters.

We found a signature of stochastic acceleration in the anticorrelation between the peak energy (E_p) of the spectral energy distribution (SED) and the spectral curvature parameter (b). We found signature of energetic budget of the jet in the correlation between the peak flux of the SED (S_p) and E_p. Moreover, using simultaneous *Swift* UVOT/XRT/BAT data, we demonstrated, that during the strongest flares, the UV-to-X-ray emission from Mrk 421 requires that the curved electron distribution develops a low energy power-law tail.

The observed spectral curvature and its anticorrelation with E_p is consistent with both stochastic acceleration or energy-dependent acceleration probability mechanisms, whereas the power-law slope of *XRT-UVOT* data is close to that inferred from the GRBs X-ray afterglow and in agreement with the *universal* first-order relativistic shock acceleration models. This scenario implies that magnetic turbulence may play a twofold role: spatial diffusion relevant to the first order process and momentum diffusion relevant to the second order process.

The Extreme sky: Sampling the Universe above 10 keV - extremesky2009,
October 13-17, 2009
Otranto (Lecce) Italy

*Speaker.

PoS(extremesky2009)039

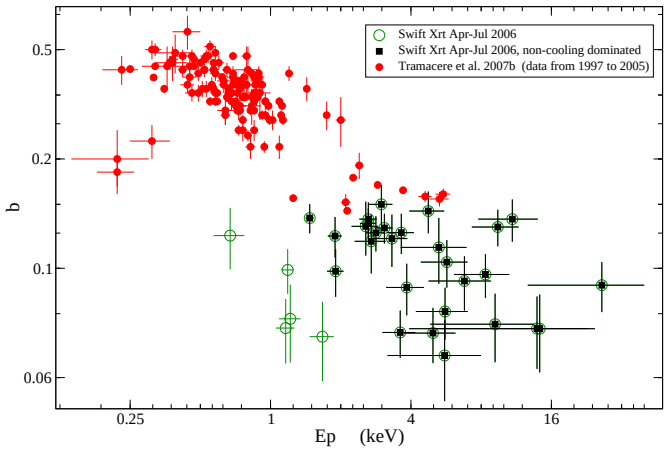

Figure 1: Scatter plot of the curvature (b) vs. E_p. Solid red circles represent data from Tramacere et al. (2007). Black boxes represent Swift data from Tramacere et al. (2009), without the cooling-dominated events. Empty circles represent the whole XRT data set presented in Tramacere et al. (2009).

1. Introduction

BL Lac objects are Active Galactic Nuclei (AGNs) characterized by a polarised and highly variable nonthermal continuum emission extending from radio to γ-rays. In the most accepted scenario, this radiation is produced within a relativistic jet that originates in the central engine and points close to our line of sight. The relativistic outflow has a typical bulk Lorentz factor of $\Gamma \approx 10$, hence the emitted fluxes, observed at an angle θ, are affected by a beaming factor $\delta = 1/(\Gamma(1-\beta\cos\theta))$.

The Spectral Energy Distribution (SED) of these objects has a typical two-bump shape. According to current models, the lower-frequency bump is interpreted as synchrotron (S) emission from highly relativistic electrons with Lorentz factors γ in excess of 10^2. This component peaks at frequencies ranging from the IR to the X-ray band. In the framework of the Synchrotron Self Compton (SSC) emission mechanism, the higher-frequency bump can be attributed to inverse Compton scattering of synchrotron photons by the same population of relativistic electrons that produce the synchrotron emission (Jones et al., 1974).

Mrk 421 is classified as a High energy peaked BL Lac (HBL) (Padovani & Giommi, 1995) because its synchrotron emission peak ranges from a fraction of a keV to several keV. With its redshift $z = 0.031$, it is among the closest and most well studied HBLs. In spring/summer 2006, Mrk 421 reached its highest X-ray flux recorded until that time. The peak flux was about 85 milli-Crab in the 2.0-10.0 keV band, and corresponded to a peak energy of the spectral energy distribution (SED) that was often at energies higher than 10 keV.

In this paper we use *Swift* UV and X-ray data (Tramacere et al., 2009) of the 2006 flaring activity, completed with historical X-ray observations, to interpret the correlation between the spectral parameters in terms of acceleration processes and energetic budget of the jet. We remand the reader to Tramacere et al. (2009) that paper for a more complete picture.

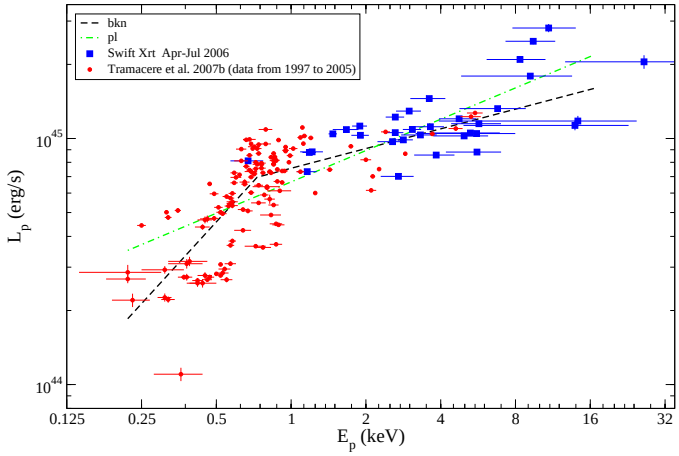

Figure 2: Scatter plot of L_p vs E_p. Solid red circles represent data from Tramacere et al. (2007) spanning from 1997 to 2005. Solid blue boxes represent Swift data from Tramacere et al. (2009). The green dashed dotted line represents the best fit using a power-law and the black dashed line represents the best fit using a broken power law.

2. Spectral parameter trends

Mrk 421 showed in the past several major flaring episodes marked by flux variations that went along with significant spectral variations (Massaro et al., 2004). The X-ray spectral shape in general exhibited a marked curvature that is described well by a log-parabolic model (Massaro et al., 2004; Tramacere et al., 2007), that can be expressed in terms of the SED peak energy (E_p), of the SED peak flux (S_p), and of the peak spectral curvature (b) as: $S(E) = S_p\ 10^{-b\ (\log(E/E_p))^2}$.
In the following we investigate the signature of stochastic acceleration in the anticorrelation between E_p and b. Moreover, we look for signatures of energetic budget of the jet in the correlation between S_p and E_p.

2.1 $E_p - b$ trend

In Fig. 1 we show the $E_p - b$ trend for both *XRT* 2006, and historical data. Thanks to the very high statistics exhibited during the 2006 flaring activity, we were able to perform an highly temporally-resolved spectral analysis and to identify cooling-dominated observations (empty circles in Fig. 1), characterized by a strong flux decrease and strong spectral softening. These cooling-dominated states are disentangled from the full dataset because they can bias the acceleration-driven trend.
The $E_p - b$ scatter plot shows a clear anticorrelation, with the peak energy of the S component increasing as its spectral curvature is decreasing. This trend hints for an acceleration processes producing curved electron distributions, where the curvature decreases as the acceleration becomes more efficient. A first possible scenario is that in which the acceleration probability of the particle is a decreasing function of its energy (Massaro et al., 2004). An alternative explanation is provided by the stochastic acceleration (SA) framework (Kardashev, 1962; Tramacere et al., 2007). In the SA mechanism the momentum-diffusion term (D) is responsible for the broadening of the electron

energy distribution ($n(\gamma)$), hence it is inversely proportional to the curvature in the observed X-ray photons (b) and to the curvature in the distribution of the emitting particles (r) . According to the relation between r and b (Massaro et al., 2004, $r \sim 5b$) we derive the following relation among the peak energy of the electron distribution (γ_p), b, and E_p:

$$\log(E_p) = 2\ \log(\gamma_p) + 3/(5b). \tag{2.1}$$

Clearly, this trend predicts the anticorrelation between E_p and b, in agreement with the observational data reported in Fig. 1.

2.2 $S_p - E_p$ trend

The $S_p - E_p$ trend (Fig. 2) demonstrates the connection between the average energy of the particle distribution and the power output of the source. To obtain a deeper understanding of the jet energetics, we plot on the y axis $L_p = S_p 4\pi D_L^2$, where $D_L \simeq 134$ Mpc is the luminosity distance[1]. In the case of synchrotron emission, we expect: $S_p \propto n(\gamma_{3p}^3) B^2 \delta^4$ and $E_p \propto \gamma_{3p}^2 B\delta$, where γ_{3p} is the peak of $n(\gamma)\gamma^3$, B is the magnetic field, and δ is the beaming factor.
It follows that the dependence of S_p on E_p can be expressed in the form of a power-law: $S_p \propto E p^{\alpha}$. The simple power-law fit gives a value of $\alpha = 0.42 \pm 0.06$, this value clearly rules out as main drivers both $B(\alpha = 2)$ and $\delta(\alpha = 4)$, indicating γ_p as the main driver.
A more detailed analysis of the scatter plot reported in Fig.2 shows that the trend has a break at about 1 keV. The broken power law fit gives two slopes of $\alpha_1 = 1.1 \pm 0.2$ and $\alpha_2 = 0.27 \pm 0.07$, respectively. This break in the trend implies that for $E_p \lesssim 1$ keV and $L_p \lesssim 10^{45}$ erg/s, the driver follows the relation with $\alpha \simeq 1.0$ (we define this state the quiescent sate), whilst for $E_p \gtrsim 1$ keV and $L_p > 10^{45}$ erg/s, the driver relates to $\alpha \simeq 0.2$ (we define this to be the high state).
A possible interpretation is that the break of $S_p - E_p$ depends on the modulation of the number of emitted particles ($N = \int n(\gamma) d\gamma$). Since B and δ have been ruled out as main drivers of the $S_p - E_p$ trend, we assume that they have a small variance. In this scenario, as γ_{3p} (namely E_p) is increasing N is constant up to a maximum value of the electron energy density $u_e = \int \gamma m_e c^2 n(\gamma) d\gamma$ corresponding to a L_p of $\simeq 10^{45}$ erg/s, that could represent the maximum energetic budget of the jet. Above the value of $E_p \simeq 1$ keV, N decreases to don't exceed the maximum energy content.

3. UV-to-X-ray spectrum and SED modelling

Combined simultaneous *UVOT* and *XRT* observations (Tramacere et al., 2009) shows SEDs (see left panel of Fig. 3) that can be classified in three categories: *a)* described by a log-parabola, *b)* described by a power law, *c)* described by a spectral law that is a power law at its low energy tail, becoming a log-parabola function at its high energy one (LPPL)
The power-law spectral index, in the $\nu F(\nu)$ representation, for model b and c were found in the range $a_\nu \simeq [0.25 - 0.4]$. According to the standard synchrotron theory, these values are not compatible with a high value of the minimum energy of the electron distribution (γ_{min}). Indeed, in this case we would expect $a_\nu \simeq 4/3$, a value much harder than the observed one. This implies a low energy power-law tail in $n(\gamma)$. Using the well known relation (Rybicki & Lightman, 1979) between

[1] We used a flat cosmology model with $H_0 = 0.71$ km/(s Mpc) $\Omega_M = 0.27$ and $\Omega_\Lambda = 0.73$.

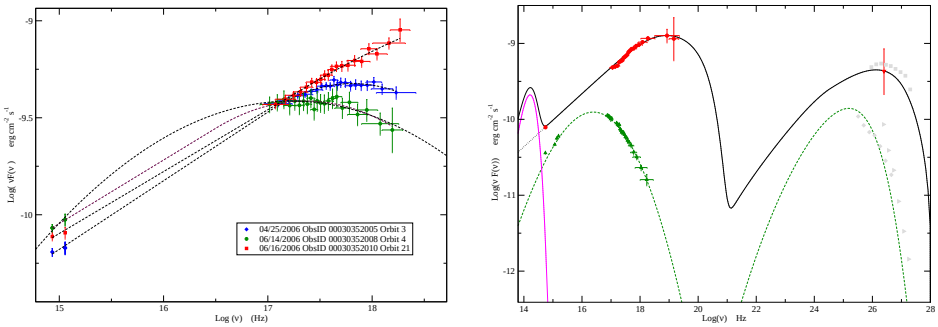

Figure 3: *Left* panel: Three different spectral shapes of the UV-to-X-ray data from Tramacere et al. (2009). Red boxes represent a PL spectrum observed on 2006 June 16. Blue diamonds represent a LPPL spectrum on 2006 April 25. Green circles represent a LP spectrum on 2006 June 14. *Right* Panel: SSC model. Solid red circles represent data from, 06/23/2006 *UVOT-XRT-BAT* observations. Green up triangles shows *UVOT-XRT* data on 03/31/2005 from Tramacere et al. (2007). Empty grey polygons represent non-simultaneous EBL corrected TeV data (Albert et al., 2007; Yadav et al., 2007). The solid red down triangle represent a *Whipple* observation on 18,19 and 21 June 2006 (Lichti et al., 2008). Best fit parameters for the 06/23/2006 state: source size $R = 2.1\times10^{15}$ cm, B=0.1 G, $\delta = 25.0$, N=15.0 cm^{-3}, s=2.3, r=0.65, γ_c=2.85×10^5.

the electron energy distribution spectral index (s) and that in the S photons ($s = 3-2a_\nu$) we obtain $s \simeq [2.2-2.5]$. A phenomenological description of $n(\gamma)$, consistent with the observed UV-to-X-ray spectrum, is given by the following spectral law:

$$\begin{aligned} n(\gamma) &= K\,(\gamma/\gamma_c)^{-s}, & \gamma \le \gamma_c \\ n(\gamma) &= K\,(\gamma/\gamma_c)^{-(s+r\ \log(\gamma/\gamma_c))}, & \gamma > \gamma_c \ , \end{aligned} \tag{3.1}$$

where r is the curvature and γ_c the turn-over energy. The presence of a power-law feature and the range of observed spectral indices are relevant both in the context of Fermi first-order acceleration models and from an observational point of view. Indeed, our range of spectral index values ($s \simeq [2.2-2.4]$) is consistent with the predictions of the relativistic-shock acceleration ($s \simeq 2.3$), both in the case of analytical or numerical approaches (Achterberg et al., 2001; Blasi & Vietri, 2005). Moreover, we note that Waxman (1997), studying the the afterglow X-ray emission of $\gamma-$ray bursts (GRB), inferred an electron distribution index of $s \simeq 2.3 \pm 0.1$. Although the emission scenarios assumed in the case of GRBs are more complex w.r.t. the one-zone homogeneous SSC model, the similar values of the electron energy spectral index hints for the relativistic-shock acceleration as an underlying acceleration mechanism common both to GRBs and HBLs. We remind that the power-law feature can also be consistent with a purely stochastic scenario, but in this case, it requires a fine tuning of the ratio of the acceleration to the loss timescale ($s \simeq 1 + t_{acc}/t_{esc}$) to get a *universal* index.

An example of SSC modelling obtained using a LPPL electron distribution is reported in the right panel of Fig. 3 (for a more detailed analysis of the SED modelling we remand to Tramacere et al. (2009)). The red points represent the simultaneous *Swift* data on 06/23/2006, and the green points data for the 31/05/2005 state. Here we just stress the huge difference in the spectral shape and flux levels between the two states. Indeed, for the 2005 data the S component is well described both in the UV and X-ray window, by using as $n(\gamma)$ a pure log-parabola. On the contrary, the 2006 state

requires a LPPL electron distribution to fit the UV-to-X-ray data. Because of the dominant galaxy contribution below UV energies, 2005 *Swift* data don't allow to understand whether or not a low energy PL feature develops. We remark that such a feature could be tested comparing the prediction from a one zone homogeneous SSC model with simultaneous *Swift* and Fermi-*LAT* MeV/GeV data.

4. Conclusion and Discussion

We have shown that the X-ray flaring activity of Mrk 421 results in a complex spectral evolutions due to drastic changes in the electron energy distribution probably related to a complex acceleration scenario. Indeed, in our analysis we found both signatures of first and second order acceleration processes acting at the same time. The $E_p - b$ trend is consistent with a SA scenario with the X-ray spectral curvature related to the acceleration rather than to the cooling process. The presence of a power-law low-energy tail, found during the brightest X-ray flares in 2006, and the corresponding values of the electron distribution index ($s \simeq [2.2 - 2.4]$) are consistent with the predictions of relativistic Fermi first-order acceleration models ($s \simeq 2.3$). Our findings hint for a simultaneous role of the first and second order processes both related to the magnetic field turbulence. The stochastic acceleration hence is related to a momentum diffusion coefficient which drives the curvature consistently with the $E_p - b$ observed trend. The first order acceleration, observationally signed by the low-energy power-law spectral index, is linked to the spatial diffusion coefficient. Interestingly, recent particle-in-cell simulations by Spitkovsky (2008) obtain electron distributions that are compatible with this scenario.
The $S_p - E_p$ trend demonstrates the connection between the average energy of the particle distribution and the power output of the source. The observed values of the expected power-law dependence ($S_p \propto E_p^{\alpha}$) exclude B, and δ, indicating γ_p as the main driver of the $S_p - E_p$ trend. The break in the $S_p - E_p$ scatter plot (see Fig. 2) at about 1 keV, where the typical source luminosity is about $L_p \simeq 10^{45}$ erg/s, can be interpreted as an indicator of the energetic content of the jet.

References

Achterberg, A., Gallant, Y. A., Kirk, J. G., & Guthmann, A. W. 2001, MNRAS, 328, 393
Albert, J., Aliu, E., Anderhub, H., et al. 2007, ApJ, 663, 12
Blasi, P. & Vietri, M. 2005, ApJ, 626, 877
Jones, T. W., O'dell, S. L., & Stein, W. A. 1974, ApJ, 188, 353
Kardashev, N. S. 1962, Soviet Astronomy, 6, 317
Lichti, G. G., Bottacini, E., Ajello, M., et al. 2008, ArXiv e-prints, 805
Massaro, E., Perri, M., Giommi, P., Nesci, R., & Verrecchia, F. 2004, A&A, 422, 103
Padovani, P. & Giommi, P. 1995, MNRAS, 277, 1477
Rybicki, G. B. & Lightman, A. P. 1979, Radiative processes in astrophysics (New York, Wiley-Interscience, 1979. 393 p.)
Spitkovsky, A. 2008, ApJ, 682, L5
Tramacere, A., Massaro, F., & Cavaliere, A. 2007, A&A, 466, 521
Tramacere, A., Giommi, P., Perri, M., Verrecchia, F., & Tosti, G. 2009, A&A, 501, 879
Waxman, E. 1997, ApJ, 485, L5+
Yadav, K. K., Chandra, P., Tickoo, A. K., et al. 2007, Astroparticle Physics, 27, 447